Three-dimensional measurement of OH-concentration gradients in a turbulent flame by simultaneous laser induced fluorescence and Raman scattering

A. Hoffmann*[,1], C. Schulz[1], J. Ruckwied[2], D. Malcherek[2], T. Dreier[2,3], R. Schießl[2], U. Maas[2]
[1]Physikalisch-Chemisches Institut (PCI)
Universität Heidelberg
Heidelberg, Germany
[2]Institut für Technische Verbrennung (ITV)
Universität Stuttgart
Stuttgart, Germany
[3]Current address: Paul Scherrer Institut (PSI)
Villingen, Switzerland

Abstract
Three-dimensional gradients of the hydroxyl radical (OH) concentration were measured in a premixed, lean natural gas / air flame by simultaneous laser induced fluorescence imaging (LIF) in a crossed-light-sheet confguration and one-dimensionally resolved Raman scattering. The technique is applied to measurements in a turbulent bluff-body flame with the aim to investigate correlations between species concentration gradients and local concentrations.

Introduction

Simulation methods for the simplified treatment of turbulent combustion like Large Eddy Simulation or probability density function (pdf) approaches rely on submodels that require information about the coupling of chemical reactions and turbulent transport [1,2]. One way to provide this information is to extract it from Direct Numerical Simulations (DNS) of turbulent flames [3,4]. Alternatively, experimental data can be used for this task.

Most of the conventional methods for obtaining this information use one- or two-dimensional visualization like Raman/Rayleigh or laser induced fluorescence (PLIF, 2D-LIF) (see, e.g. [5-7]). These methods, however, merely provide linear or planar cross-sections through the observed object. They can therefore not distinguish between isolated areas (i.e. "islands" of burning gases) and structures that are connected via the third dimension. The information of the propagation of a structure perpendicular to the measured plane is missing. Furthermore, gradients measured by these planar techniques are only a projection of the real gradients onto the observed line or plane. However, if the measured information is to be used as an input for turbulent combustion models, the three-dimensional structure of turbulent flames must be taken into account [8]. The need for an instantaneous 3D imaging-technique is therefore obvious.

Requirements for combustion modeling

Turbulent premixed flames are quite complex to treat in numerical simulations due to the large amount of variables that need to be calculated, and due to the large span of temporal and spatial scales that have to be resolved in order to perform a detailed simulation. It is therefore advisable to identify *correlations* between several quantities, like for instance species concentrations, temperature or gradients of these quantities, in order to simplify the description and numerical simulation of such flames. Specifically, links (correlations) between spatial concentrations and their spatial gradients can lead to the closure of molecular transport terms in the pdf transport equation [9].

An appropriate flame for testing the validity of the simulation approach is a turbulent, premixed natural gas/air flame; this type of flame is a quite realistic model of the combustion process found in technical devices (e.g., in gas-turbines). By using a bluff-body flame stabilisation rather than a piloted flame, the simulation of combustion system is more difficult; therefore such a flame provides a more sensitive test case for checking the validity of the employed models.

3D imaging approaches

For instantaneous observation of three-dimensional structures in turbulent flows several approaches have been developed and applied to turbulent mixing processes and flames. Parallel alignment of multiple detection planes either using subsequent detection of the imaged planes with a single camera and sweeping long pulse or cw-laser beams and scanning mirrors or using high repetition rate imaging with the need of laser- and camera-"clusters" was used to observe volumes within turbulent flows [10-13]. These techniques can visualize extended areas within the flow field. The spatial resolution in the *z*-dimension (perpendicular to the observed planes), however, is rather low. An alternative

* Corresponding author: Axel.Hoffmann@pci.uni-heidelberg.com
Associated Web site: http://www.pci.uni-heidelberg.de/pci/
Proceedings of the European Combustion Meeting 2003

attempt to image 3-dimensional volume elements is the use of crossed detection planes [14-17]. A quasi-instantaneous detection is provided with two cameras. In special mirror arrangements the detection is possible with a single laser and camera only [18]. One of the benefits of this method is the increasing resolution towards the crossing line and a small cylindrical volume of several hundred micrometers to approximately 1 mm around it. This geometry is ideal for the combination with 1D-Raman line measurements which can provide temperature profiles and multi-species distributions in a limited part of the crossing line [19]. We apply this technique for measuring OH concentrations and OH concentration gradients along with temperature and majority species concentrations.

Experimental setup

The arrangement of the laser beams in the observed volume is shown in fig. 1. A tunable KrF excimer laser (Lambda Physik, EMG150TMSC, 160 mJ per pulse, 0.5 cm^{-1} full width at half maximum) is tuned to 248.450 nm to excite in the $P_2(8)$ transition within the A-X (3,0) band of OH. The laser beam is split into two beams by a 50% beam splitter. One of the beams is directed through a Dove prism to turn the rectangular beam profile by an angle of 45°. Via dielectric mirrors this beam is directed through the detection volume passing one cylindrical lens ($f = 1500$ mm) to form a thin (300 µm thick) laser light sheet. The second part of the beam passes a second Dove prism that allows to adjust the laser beams independently to the crossing angle of 90°. An arrangement of dielectric mirrors delays this part of the beam by 70 ns (27 m optical delay line) in order to allow selective detection of the signal of both planes and a set of sheet forming lenses to cross the first beam in the detection volume in the desired way. The lens set also consists of a $f = 1500$ mm cylindrical lens for the focusing of the sheet but also of an additional $f = 2000$ mm lens to compensate for beam divergence. The light sheet is focused to the same thickness (300 µm). The arrangement of prisms and mirrors reduces the laser intensity by approximately 30% for the direct beam and up to 70% for the delayed beam. The resulting laser power densities in the observed region are approximately 300 MW/cm^2.

The OH LIF signal emitted from the A-X (3,2) band is separated from interfering signal contributions with reflection band pass filters (Laser Optik, 295±10 nm) and focused (Halle, UV lens, $f = 300$ mm, $f_\# = 5.0$) onto two intensified CCD-cameras (LaVision, StreakStar) One camera is detecting in a top down direction, the other one observes the illuminated region via an UV-coated aluminum mirror in a bottom up direction.

The crossing line of the two laser light sheets coincides with the pulse-stretched beam of a frequency doubled Nd:YAG laser system (two BMI 5022 DNS 10, nominal pulse energy 600 mJ each, pulse duration 6 ns, emission wavelength 532 nm). Raman scattering from this line is imaged with an achromatic lens (LINOS, aperture 210 mm, $f_\# = 4$) onto the slit of a Czerny-Turner type spectrometer (ARC, $f_\# = 4$, focal length 300 mm, slit width 500 µm, 600 grooves/mm grating). The output of the spectrometer is a spatially resolved Raman spectrum emitted from a cylindrical volume within the flame, with a length of 3.2 mm and a diameter of 300 µm. By capturing this signal with an intensified CCD camera, a record of the thermochemical state of the measurement volume is obtained for each position along the illuminated line, containing information about temperature as well as species mole fractions for CO_2, O_2, CO, N_2, CH_4 and H_2O. In order to increase the signal-to-noise ratio, the information from 250 individual pixels along the spatial direction is binned together into groups of 10 pixels, such that 25 distinct spatial points are recorded, corresponding to a nominal spatial resolution of 130 µm in direction of the laser beam axis.

Both diagnostics systems, Raman and the two LIF cameras with the appropriate laser beams are synchronized within a 350 ns period to ensure quasi-simultaneous measurements. The complete experimental setup of the Raman system on the one hand and the LIF setup on the other hand is depicted in fig. 3.

The investigated flame (fig. 2) was generated by a bluff-body stabilized, premixed, turbulent, non-swirling natural gas/air burner. This burner features an air coflow

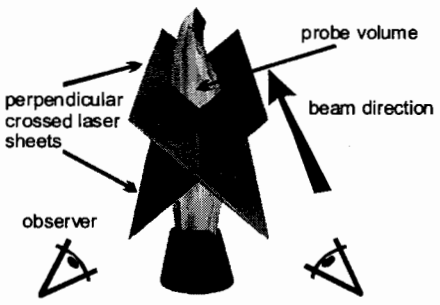

Fig. 1: Detection principle for the 3D measurement using crossed laser light sheets. The crossing line of the light sheets coincides with the volume observed by 1D-Raman scattering.

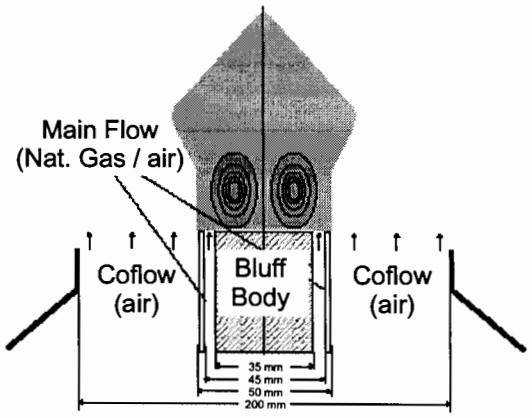

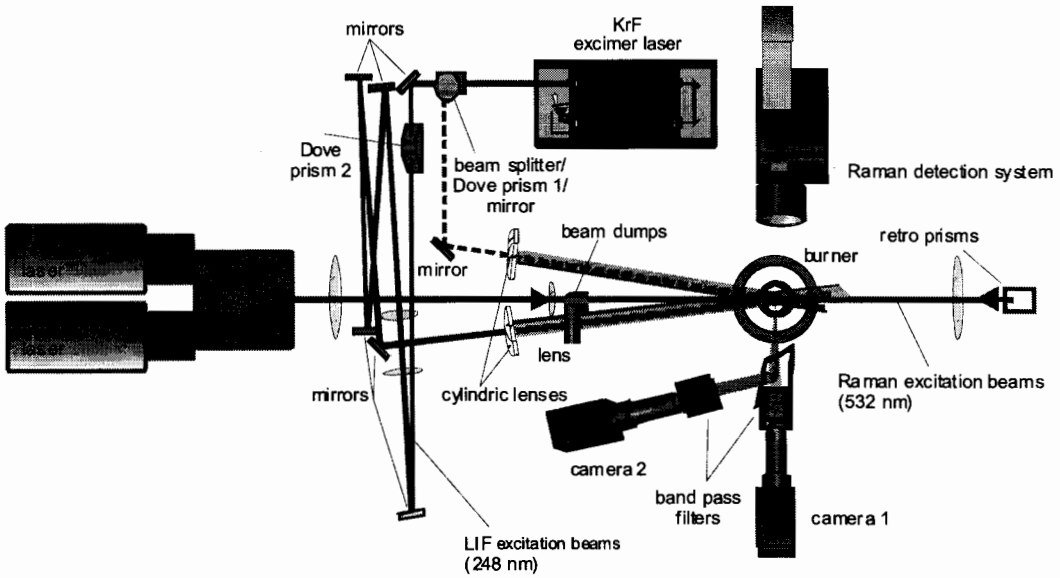

Fig. 3: Experimental setup of the simultaneous Raman/LIF measurements.

to suppress turbulent shear layers on the flame boundary and to provide a particle-free environment for laser-based measurements. The burner head consists of a cylindrical, vertically aligned metal-tube, with a cylindrical bluff-body aligned in the center. A natural gas/air mixture is flowing from the gap between the tube and the bluff-body (55 m³/minute, equivalence ratio $\Phi = 0.95$), which burns after mixing with a recirculating vortex of hot burned gases. The Reynolds number of the cold flow is about 15000. The flame is statistically axisymmetric, and the visible flame cone is about 50 cm high. There is considerable entrainment of air in the upper part of the flame. The burner has been characterized well by previous measurements and has also been subject of numerical studies using a pdf-approach [20].

The flame is mounted on a xy traversing system, so that measurements at arbitrary points in the flame are possible.

The positions measured during this work cover a range from 20 to 80 mm height above the burner nozzle and radial positions from 0 to 14 mm distance from the burner axis. The data presented here were measured 40 mm above the nozzle at a radial position of 14 mm.

To ensure correct alignment and superposition of the measured data a marked target is used which allows to correct for distortions and relative sizing of the measured OH-LIF images. The laser intensity variation within the light sheets was measured by detecting toluene LIF in a homogeneously seeded air flow. For calibration a McKenna burner was used to calibrate temperature and OH number densities. Unfortunately, the spatial properties of the McKenna burner do not allow optical access to the detection area of the lower camera. For this reason additional measurements were carried out in a modified Taran burner, which could be installed in the setup, to correct the intensity values of both images.

Data reduction

After determination of the position of the intersection line in both images and the selection of the region of interest, which is the region near the flame front, the images with a size of about 100 by 40 pixels (12 x 5 mm) are written into a 3D matrix as shown in fig. 4.

To fill the area of missing information in the volume outside the crossed laser-sheets, a diffusion algorithm is applied [18]. This algorithm uses the measured image gray values along the two perpendicular laser sheets, and sequentially applies a diffusion-like operation to

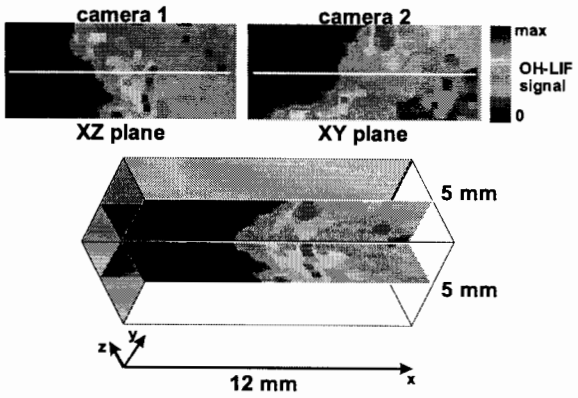

Fig. 4: Upper frames: selected sections from the measured image pair. Below: 3D volume with the two source planes. The line marks position of the cutting line. The height is 40 mm above the burner nozzle, radial position is 14 mm from the burner axis.

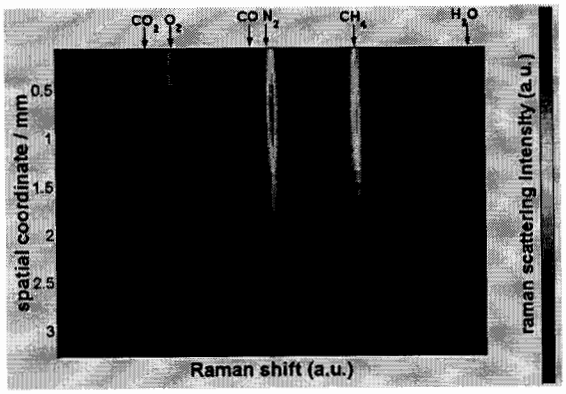

Fig. 5: A typical image of a spectrally and spatially resolved single-shot Raman signal. False color codes indicate signal intensities.

promote this information into the close region around the intersection line. The gray values in the crossed planes are kept constant during the diffusion process.

Now, in the completely filled volume the derivatives in all three spatial directions can be evaluated separately. Finally, the gradient information in three spatial directions allows us to evaluate the absolute values of the 3-dimensional gradients in the cutting line. We have to keep in mind that the resolution of the gradients is highest in the proximity of the cutting line.

For the Raman measurements, the desired information, namely spatial profiles of temperature and species mole fractions, has to be extracted from the recorded Raman-images. These can be represented by matrices ($S_{i,j}$), where $S_{i,j}$ denotes the gray value of the pixel with row- and column- index i and j, respectively. According to the properties of our setup, i and j are associated with spatial location and Raman emission wavelength, respectively (cf. fig. 5). The image matrix ($S_{i,j}$) is related to the spatial profiles of temperature and mole fractions via equations of the form

$$S_{i,j} = \sum_k p/(RT_i)\, x_{i,k}\, f_{i,j,k}(T_i) \qquad (1)$$

where p is the absolute pressure, R the molar gas constant, and T_i the temperature at a location identified by i. $x_{i,k}$ denotes the mole fraction of the k^{th} species ($k = CO_2, O_2, CO, N_2, CH_4, H_2O$) at i. The pressure was assumed to be spatially and temporally invariant, which is certainly realistic for the conditions of our experiment. $f_{i,j,k}(T_i)$ is a function that describes how the spectral emission feature of species k (normalized to mole fraction 1) is converted to ICCD camera readings. This function therefore combines parameters related to molecular properties (temperature dependence of Raman cross sections and of spectral emission line shape) and to features of the experimental setup like pump laser intensity, light collection efficiency of the employed detection line, and the like. $f_{i,j,k}$ was found by calibration procedures, which were supported by a modification of the computer program RAMSES [21] for Raman spectra simulation. Assuming that at every spatial location (index i) the mole fractions of the detected species sum up to 1,

$$\sum_k x_{i,k} = 1 \qquad (2)$$

and using eq. (1), a nonlinear equation system is obtained, which can be solved for $T_{i,k}$ and $x_{i,k}$, thus allowing for the determination of spatial profiles of temperature and mole fractions from the measured signal ($S_{i,j}$). The Gauss-Newton type solver NLSCON [22] was used to solve the equation system numerically.

Results

The temperature information from the simultaneous Raman experiments allows the quantification of the LIF signal, and absolute OH concentrations can be calculated. A sample Raman result is shown in fig. 6. The different measured scalars, temperature and major species mole fractions are plotted. These data can be directly compared and correlated to the measured 3D gradients of OH number densities. The data in fig. 6 feature a nice example of the importance of three dimensional information: The raman traces show an

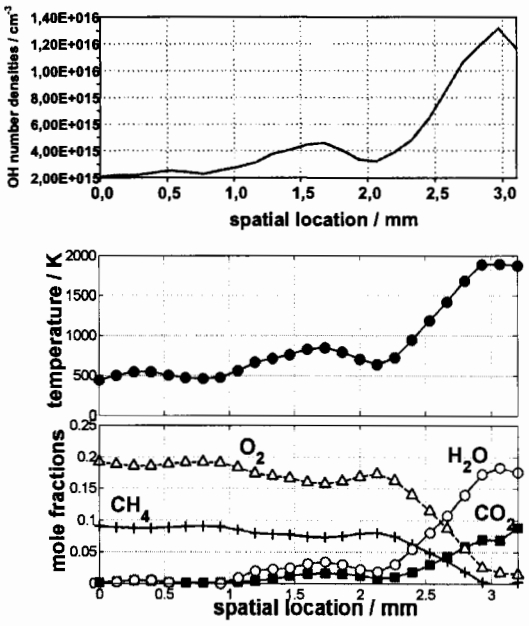

Fig. 6:
Top: Plot of OH number densities (in cm^{-3}),
Middle: simultaneous temperature profile
bottom: species mole fractions

increase in temperature and a decrease of O_2 and CH_4 mole fractions in the unburned zone between 1mm and 2mm along the profile. In the very same zone, the OH LIF intensity also increases. From the 1D-information shown in fig. 6, this behaviour appears rather strange; from the 3D information provided by the crossed-plane OH LIF images, it is clearly seen that a flame front partially "touches" the laser-beam from the side, a fact

which explains the shape of the 1D-profiles in fig. 6 very well.

Fig. 7: Absolute values of the 3D gradients in the source planes evaluated from the individual derivatives of the three spatial directions. The white lines indicate the location of the crossing line.

Fig. 7 shows the result of the gradient evaluation from the 3D matrix. The visualized planes in pictures are the results from the original source planes. But also in the next proximity to the cutting line highly resolved gradient information is available from the matrix volume.

The direct comparison of gradients obtained from planar measurements with those evaluated from the 3D dataset is shown in fig. 8. It shows that the use of 2-dimensional information only can be misleading as spatial structures in turbulent flames expand in all 3

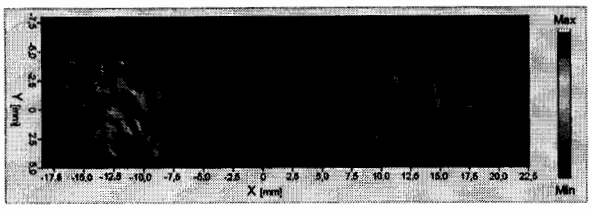

Fig. 9: 3D view of OH-LIF intensities in a Bunsen burner flame by means of volume visualization. The dark zone in the middle is the fresh gas flow.

spatial directions. A simple planar observation of the object does not take this into account.

With the available data in the 3D matrix it is possible by means of volume visualization to calculate a perspective view of the investigated volume. Fig. 9 shows a 3D view of a Bunsen burner flame which was investigated in our former experiments.

Conclusions

We have presented an approach for the simultaneous measurement of scalars and concentration gradients in a turbulent, premixed, lean methane/air flame. Beside temperature and species concentrations, magnitude and direction of spatial gradients of the hydroxyl-radical concentration was measured in three dimensions. The measured data provide a large database of simultaneous multi-scalar and gradient information along a line in different regions of the flame. The statistical evaluation of these data is in progress; the results will aid in solving certain problems of turbulent reactive flows, like the closure problem of transport terms in pdf-models.

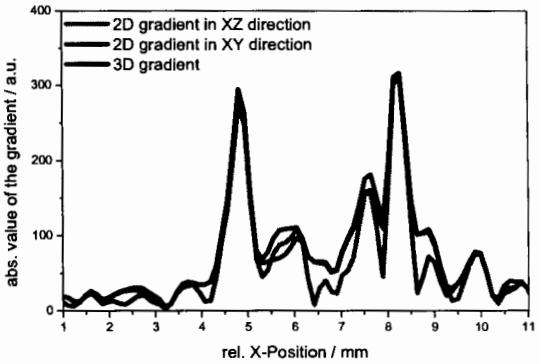

Fig. 8: Comparison of 2D gradients in the crossed planes with the gradient evaluated from the 3D data set.

Acknowledgements

The financial support by the Deutsche Forschungsgemeinschaft is gratefully acknowledged. Thanks are also due to the Konrad-Zuse Institut für Informationstechnik, Berlin, for providing the public-domain equation solver NLSCON.

References

1. Pope, S. B. "Computation of turbulent Combustion: Progress and Challenges," in *Proceedings of the Combustion Institute 24* (University of Sydney, Australia, 1990), 591.
2. Borghi, R., *Progress in Energy and Combustion Science* 14:245-292 (1988).
3. Peters, N. "Laminar Flamelet Concepts in Turbulent Combustion," in *Proceedings of the Combustion Institute 21* (Munich, Germany, 1986), 1231-1250.
4. Reynolds, W. C., "The potential and limitations of direct and large eddy simulation," in *Whither Turbulence? Turbulence at the crossroads, Lecture Notes in Physics* (Springer, New York, 1989), p. 313.
5. Paul, P. H. and Najm, H. N. "Planar Laser Induced Fluorescence Imaging of flame heat release rate," in *Proceedings of the Combustion Institute 27* (Boulder, CO, 1998), 43-50.
6. Cabra, R., Myhrvold, T., Chen, J. Y., Dibble, R. W., Karpetis, A. N., and Barlow, R. S. "Simultaneous Laser Raman-Rayleigh-LIF Measurements and Numerical Modeling Results of a Lifted Turbulent H_2/N_2 Jet Flame in a Vitiated Coflow," in *Proceedings of the Combustion Institute 29* (Hokkaido University , Sapporo, Japan, 2002), 1881-1888.
7. Kalt, P. A. M., Al-Abdeli, Y. M., Masri, A. R., and Barlow, R. S. "Swirling Turbulent Non-Premixed Flames of Methane, Flow Field and Compositional Structure," in *Proceedings of the Combustion Institute 29* (Hokkaido University , Sapporo, Japan, 2002), 1913-1919.

8. Thévenin, D., Gicquel, O., De Charentenay, J., Hilbert, R., and Veynante, D. "Two- versus three- dimensional direct simulations, of turbulent methane flame kernels using realistic chemistry," in *Proceedings of the Combustion Institute 29* (Hokkaido University , Sapporo, Japan, 2002), 2031-2039.
9. Warnatz, J., Maas, U., and Dibble, R. W., *Combustion*, 3rd ed (Springer, 2002).
10. Yip, B., Fourguette, D. C., and Long, M. B., *Applied Optics* 25:3919-3923 (1986).
11. Landenfeld, T., A., Kremer, Hassel, E. P., Janicka, J., Schäfer, T., Kazenwadel, J., Schulz, C., and Wolfrum, J., *Proc. Combust. Inst.* 27:1023-1030 (1998).
12. Nygren, J., Hult, J., Richter, M., Aldén, M., Christensen, M., Hultqvist, A., and Johansson, B. "Three-dimensional laser induced fluorescence of fuel distributions in an HCCI engine," in *Proceedings of the Combustion Institute 29* (Hokkaido University, Sapporo, Japan, 2002), 679-685.
13. Frank, J. H., Lyons, K. M., and Long, M. B., *Optics Letters* 16:958-960 (1991).
14. Knaus, D. A., Gouldin, F. C., Hinze, P. C., and Miles, P. C., *SAE Technical Paper Series No. 1999-01-3543* (1999).
15. Knaus, D. A. and Gouldin, F. C. "Measurement of flamelet orientations in premixed flames with positive and negative Markstein numbers," in *Proceedings of the Combustion Institute 28* (Edinburgh, Scotland, 2000), 367-373.
16. Sattler, S. S., Gouldin, F. C., and Boertlein, N. T. "Combined crossed-plane imaging and stereo-particle image velocimetry," in *Third Joint Meeting of the U.S. Sections of the Combustion Institute* (Chicago, IL, 2003).
17. Knaus, D. A., Gouldin, F. C., and Bingham, D. C., *Combustion Science and Technology* 174:101-134 (2002).
18. Hoffmann, A., Zimmermann, F., and Schulz, C. "Instantaneous three-dimensional visualization of concentration distributions in turbulent flows with a single laser," in *First International Conference on Optical and Laser Diagnostics* (City University, London, UK, 2002), in press.
19. Karpetis, A. N. and Barlow, R. S. "Measurements of flame orientation and scalar dissipation in turbulent hydrocarbon flames," in *Third Joint Meeting of the U.S. Sections of the Combustion Institute* (Chicago, IL, 2003).
20. Bender, R., Steiner, B., Schmidt, D., Schießl, R., Dreier, T., and Maas, U. "Experimentelle Untersuchung und pdf-Simulation turbulenter Vormischflammen," in *16. TECFLAM Seminar* (2002), 43-61.
21. Hassel, E. and et al., *Applied Optics* 32 (1994).
22. Nowak, U. and Weimann, L., "A Family of Newton Codes for Systems of highly nonlinear equations - Algorithm, Implementation, Application" . *ZIB* Technical Report TR 90-10 (1990).